

Article

Measuring Performances of a White-box Approach in the IoT Context

Daniele Giacomo Vittorio Albricci ¹, Michela Ceria ² , Federico Cioschi ³, Nicolò Fornari ⁴, Arvin Shakiba ⁵ and Andrea Visconti ^{6,*} 

¹ Department of Computer Science, Università degli Studi di Milano, via Celoria 18, 20133, Milan, Italy; daniele.albricci@studenti.unimi.it

² Department of Computer Science, Università degli Studi di Milano, via Celoria 18, 20133, Milan, Italy; michela.ceria@gmail.com

³ Department of Computer Science, Università degli Studi di Milano, via Celoria 18, 20133, Milan, Italy; federico.cioschi@studenti.unimi.it

⁴ Open Systems AG, Räfelfstrasse 29, 8045 Zurich, Switzerland; nforinari@open-systems.com

⁵ Department of Computer Science, Università degli Studi di Milano, via Celoria 18, 20133, Milan, Italy; arvin.shakiba@studenti.unimi.it

⁶ Department of Computer Science, Università degli Studi di Milano, via Celoria 18, 20133, Milan, Italy; andrea.visconti@unimi.it

* Correspondence: andrea.visconti@unimi.it (A.V.)

Version September 2, 2019 submitted to Symmetry

Abstract: Internet of Things refers to all the smart objects that are connected to other objects, devices or servers and that are able to collect and share data, in order to “learn” and improve their functionalities. Smart objects suffer from lack of memory and computational power, since they are usually lightweight. Moreover, their security is weakened by the fact that smart objects can be placed in unprotected environments, where adversaries are able to play with the symmetric-key algorithm used and the device on which the cryptographic operations are executed. In this paper, we focus on a family of white-box symmetric ciphers SPNbox, extending and improving our previous paper on the topic presented at WIDECOM2019. We highlight the importance of white-box cryptography in the IoT context, but also the need to have a fast black-box implementation (server-side) of the cipher. We show that, modifying an internal layer of SPNbox, we are able to increase the key length and to improve the performance of the implementation. We measure these improvements (a) on 32/64-bit architectures and (b) in the IoT context by encrypting/decrypting 10,000 payloads of lightweight messaging protocol MQTT.

Keywords: symmetric cryptography; IoT; MQTT; white-box approach; the SPNbox family

1. Introduction

The name *Internet of Things* (IoT), coined by the MIT researcher Kevin Ashton [1], usually refers to *smart objects*, connected through the Internet to other sensors, devices and servers with which collect and/or share data for improving their functionalities. IoT can also be combined with other technologies, for example with cloud computing [2]. It is possible to create a sustainable smart home aiming to reduce resources’ consumption or develop specific applications in the medical field [3] such as wearable devices which monitor our physical conditions, specific devices used to check patients with chronic illnesses, and so on. Data collected by IoT devices need to be (a) processed to form informations by applying, for example, data mining techniques [4]; (b) evaluated in order to make decision by adopting agent based models [5,6], bayesian decision models [7], fuzzy logic [8] and so on; (c) protected from attacks, failures and leaks during communication [2].

26 Several issues have to be faced in securing IoT applications. An important example is given by
27 the intrinsic constraints of the devices [9], that usually have a small amount of memory and cannot
28 perform heavy computations. It is very likely to have such devices in non-protected environment,
29 where an adversary can access them and perform attacks. In particular, she/he can perform an analysis
30 of the controlled binary [10] or perform differential fault analysis [11,12]. Moreover, since these devices
31 are connected, compromising one of them can open the way to botnet attacks [2,3]. We can observe that
32 we are exactly in a white-box framework, and white-box cryptography [13] has been first developed to
33 cope with the scenario in which an attacker can physically interact both with the implementation of the
34 used cryptographic algorithm and with the device on which the encryption/decryption operations are
35 executed. The usually studied scenario, namely black-box, in which the execution cannot be observed
36 nor modified by the attacker, is not always suitable for IoT applications [14]. The reader can think
37 about what happens in the context of digital rights management where discovering the key means to
38 have the possibility to spread digital contents to people that have not paid such contents.

39 The effort of researchers towards white-box cryptographic schemes materialized with [15] and
40 [13] where white-box versions of AES and DES have been implemented. Nevertheless, it is important
41 to remark that these implementations have been attacked via algebraic attacks [16] (improved by [17])
42 ,[18],[19], [20]. Moreover, also [21] can easily break Chow's implementations.

43 The need to have white-box algorithms for practical applications leads to develop some specific
44 algorithms. Examples of block ciphers developed to be employed in the framework of white-box
45 cryptography are ASASA [22] and SPACE [23]. However, these ciphers are not free of drawbacks or
46 weaknesses. In particular, decomposition attacks can affect ASASA's security while SPACE is heavy
47 from a computational point of view [24]. An important step forward for white-box cryptography, was
48 the development of SPNbox [24], another block cipher that relies on internal block ciphers with the aim
49 to reduce the computation time. In [9], the problem of intrinsic constraints on computational power
50 and memory of IoT devices in unprotected environment is addressed. The authors refer to smart
51 objects with limited computational power and memory that may contain sensitive data and can be
52 easily lost or stolen. Differently from AES/DES white-box implementations, the authors do not decline
53 a well-known cipher into the new framework, but they develop a new one, relying on a modification
54 of Lai-Massey structure. The crucial point is that only the encryption is thought to be done on the
55 IoT constrained device, while the decryption phase is supposed to be done on a computer or server
56 and in a black box scenario. In [25] the authors refer to embedded distributed devices which collect
57 and securely send information to centralized servers. Subsequently, these servers decrypt and process
58 all the information. As previously mentioned, the collected information may be sensitive and it is
59 possible for an attacker to get control of the whole device. The scheme proposed in [25] is lightweight
60 and suitable for constrained devices. In particular, such a new design has the following peculiarities:

- 61 • the employed operations are very simple; they essentially consist of lookup tables and bit
62 operations;
- 63 • the lookup tables and the structure containing sensitive data are small in memory;
- 64 • the provided security is medium-level ($\sim 2^{63}$) and protection is ensured for reasonable amount of
65 time;
- 66 • it is possible to update the key at small costs.

67 The scheme is based on a Fesitel structure, but it adds two bijections, as a defence against attacks.
68 Moreover, to cope with structural cryptanalysis [25,26] different size components are used.

69 This paper improves of a previous work entitiled "White-box Cryptography: A Time-security
70 Trade-off for the SPNbox Family" [27], presented by F.Cioschi, N.Fornari and A.Visconti at the
71 2nd International Conference on International Conference on Wireless, Intelligent and Distributed
72 Environment for Communication (WIDECOM 2019). In this paper, we (a) introduce the white-box
73 approach in the IoT context, explaining the importance of protecting data in an environment where
74 attackers have full control over the whole system; (b) explain the importance of having a fast black-box
75 implementation of a white-box cipher; (c) summarize our previous idea [27] explaining how to modify

76 the internal block ciphers of the SPNbox family in order to increase the size of the key space; (d)
 77 measure the performance of a black-box implementation (server-side) on 32- and 64-bit architectures
 78 and by encrypting/decrypting 10,000 payloads of a lightweight messaging protocol — i.e., MQTT —
 79 which contains the data sent over the Internet.

80 The remainder of the paper is organized as following. In Section 2, block ciphers are introduced.
 81 In Section 3, we present several white-box implementations and related attacks published in literature.
 82 In Section 4 and 5, we summarize two block ciphers' families, namely, SPACE and SPNbox, which are
 83 white-box friendly by design. In Section 6, we explain the importance of increasing the number of bits
 84 of the key used in each round. In Section 7, the testing activities are presented. Finally, Section 8 is
 85 devoted to discussion and conclusions.

86 2. Block ciphers

87 There exist two main families of block ciphers: substitution-permutation network (SPN) and
 88 Feistel network. The main difference between them is that Feistel networks play only with one half of
 89 the cipher state in each round.

90 2.1. Substitution-Permutation Networks

91 A substitution-permutation network (SPN) is a design for block ciphers proposed by Shannon in
 92 [28], where he suggested to use multiple mixing layers interleaving substitutions and permutations.
 93 Although weak on its own, applying substitutions and then permutations presents good "mixing"
 94 properties. Substitutions contribute to local *confusion* and permutations spread such a local confusion
 95 to the more distant subblocks, thus providing *diffusion* [28]. If a single input bit is flipped, it affects the
 96 m output bits of a specific S-box which, subsequently, are sent to different S-boxes by a permutation.
 97 Considering the output of such a network, about fifty percent of the bits are affected by this change.
 98 Therefore an outcome of a single bit change at the input is difficult to predict, especially if the bit of the
 99 secret key are XORed into the block between the encryption layers. In order to get better diffusion
 100 properties, several block ciphers adopt linear (as in the case of AES) or affine mappings instead of
 101 permutations.

Definition 1. Let $\phi : (\mathbb{F}_2)^r \times (\mathbb{F}_2)^l \rightarrow (\mathbb{F}_2)^r$, with $r = bt$ be a block cipher with N rounds. Let $k \in (\mathbb{F}_2)^l$ be
 the cipher key and $(k^{(0)}, \dots, k^{(N)})$ be the $N + 1$ round keys generated by k through the key schedule.
 Then ϕ is an SPN block cipher if

$$\phi_k(x) = \tau_N \circ \tau_{N-1} \circ \dots \circ \tau_0(x) \quad x \in (\mathbb{F}_2)^r$$

102 where $\tau_i = \sigma_{k^{(i)}} \circ \lambda^{(i)} \circ \gamma^{(i)}$ and

- 103 • $\gamma^{(i)} : (\mathbb{F}_{2^t})^b \rightarrow (\mathbb{F}_{2^t})^b$ is a non linear substitution
- 104 • $\lambda^{(i)} \in \text{AGL}((\mathbb{F}_2)^r)$ where $\text{AGL}((\mathbb{F}_2)^r)$ is the subgroup of the affine transformations of $(\mathbb{F}_2)^r$
- $\sigma_{k^{(i)}}$ is the addition with the round key

$$\begin{aligned} \sigma_{k^{(i)}} : (\mathbb{F}_2)^r &\rightarrow (\mathbb{F}_2)^r \\ x &\mapsto x \oplus k^{(i)} \end{aligned}$$

105 where by \oplus we denote the bitwise addition (XOR)

106 2.2. Feistel networks

107 A Feistel network is a block cipher introduced by H. Feistel and D. Coppersmith in 1973 [29]
 108 which has the advantage of having the encryption and decryption functions almost identical, making
 109 the implementation easier and cheaper compared to translation based ciphers.
 110 Let us define the following functions before describing the encryption process.

Definition 2. Let π_t be a projection, with $t \in \{1, \dots, 2n\}$, defined as:

$$\begin{aligned} \pi_t : \quad \mathbb{F}^{2n} &\rightarrow \mathbb{F}^t \\ (x_1, \dots, x_{2n}) &\mapsto (x_1, \dots, x_t) \end{aligned}$$

111 Considering $x \in \mathbb{F}^{2n}$ as a vector of bits, we can use projection π_t to choose the t most significant bits of
112 x .

Definition 3. Let q_t be a projection, with $t \in \{1, \dots, 2n\}$, defined as:

$$\begin{aligned} q_t : \quad \mathbb{F}^{2n} &\rightarrow \mathbb{F}^t \\ (x_1, \dots, x_{2n}) &\mapsto (x_{2n-t+1}, \dots, x_{2n}) \end{aligned}$$

113 In the same way, using projection q_t we can choose the t least significant bits of x .

114

115 Given $m \in \mathbb{F}^{2n}$ (a message) and $k \in \mathbb{F}^l$ (a secret key), for some positive integer l , the encryption process
116 works as follows:

- 117 1. $N + 1$ round keys k_0, \dots, k_N are generated from k by means of the key schedule
2. message m is split into a left block and right block, initialized as

$$L_0 = \pi_n(m) \quad R_0 = q_n(m)$$

3. for $i \in \{1, \dots, N + 1\}$ the round function is applied in the following way:

$$L_i = R_{i-1} \quad R_i = L_{i-1} \oplus F(R_{i-1}, k_{i-1}) \quad (1)$$

- 118 4. final ciphertext c is (R_{N+1}, L_{N+1}) .

Encryption and decryption only differ in the reverse order of the round keys, as a matter of fact the decryption of ciphertext (R_{N+1}, L_{N+1}) is accomplished computing for $i \in \{N, N - 1, \dots, 0\}$

$$R_i = L_{i+1} \quad L_i = R_{i+1} \oplus F(L_{i+1}, k_i) \quad (2)$$

119 An advantage of Feistel networks is that Feistel function F is non-necessarily invertible. This can
120 be clearly seen by analyzing how encryption and decryption work (see Equations 1 and 2).

121 3. The White-Box approach

122 The White-Box approach aims to avoid key recovery attacks by embedding the cryptographic key
123 into a robust representation of the cipher. Consider a block cipher ϕ . We compute a map $\psi : \mathbb{F}^n \rightarrow \mathbb{F}^n$
124 such that, given a key $\bar{k} \in \mathbb{F}^l$, it holds $\phi(x, \bar{k}) = \psi(x) \quad \forall x \in \mathbb{F}^n$. If an attacker knows even both ϕ and ψ ,
125 it should be very hard for him to find out the key.

Example 1. Let ϕ and ψ be defined as follows:

$$\begin{aligned} \phi(x) &:= k + x \pmod{4} & x &\in \{0, \dots, 3\} \\ \psi(x) &:= S[x] & S &= [3, 0, 1, 2] \end{aligned}$$

126 If $k = 3$, we can consider ψ as a white-box implementation of ϕ , by representing ψ as a lookup table.

127 The first white-box AES implementation has been proposed by Chow et al. in [13]. The authors
128 suggest that key extraction can be avoided by a careful use of lookup tables. In particular, given
129 a secret key and a block cipher, it is possible to create a lookup table which maps the plaintext in
130 a corresponding ciphertext. In some cases, this lookup table may be huge and unusable due to its

131 dimension. Therefore, a block cipher ϕ can be represented as a network of smaller lookup tables (see
 132 Figure 1) that have to be read in a particular order [13]. Unfortunately, in the white-box framework an
 133 adversary has full access to these tables, exposing the cipher to possible attacks. Since there is no reason
 134 to make an attacker's life easier, tables can be protected by means of internal encodings [13]. This
 135 means that a map is composed after table i and its inverse before table $(i + 1)$, leaving the ciphertext
 136 unchanged. However, internal encoding does not protect against code-lifting attacks. Indeed, an
 137 attacker may recover the tables of the cipher and understand their concatenation order. Doing so,
 138 she/he is able to decrypt messages even though he had not recovered the secret key. Therefore, another
 139 protection is required: external encoding. Internal and external encodings are also discussed in [30],
 140 while a different approach, based on polynomial algebra techniques [31], gave rise to a perturbed
 141 white-box implementation of AES [32], broken by [33] in 2010.

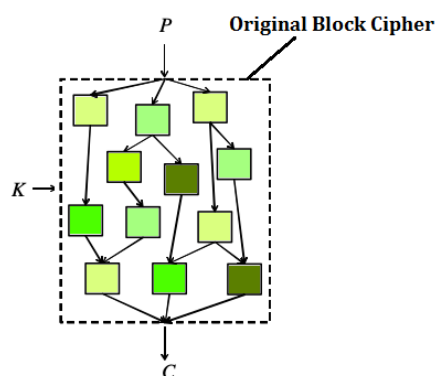


Figure 1. Table-based white-box implementation: the key k is scrambled by a network of lookup tables

142 Chow's work is a milestone for white-box cryptography and its framework has also been used by
 143 some subsequent works such as [34] and [35]. However, researchers found attacks also for these new
 144 approaches:

- 145 • White-Box AES Implementation: Chow [13]; Attack: [16]; Work Factor: 2^{30} ;
- 146 • White-Box AES Implementation: Karroumi [34]; Attack: [18] and [20]; Work Factor: 2^{22} ;
- 147 • White-Box AES Implementation: Xiao Lai [35]; Attack: [18]; Work Factor: 2^{32} ;
- 148 • White-Box AES Implementation: Xiao Lai [35] generic linear version; Attack: [18]; Work Factor:
 149 2^{38} ;
- 150 • White-Box AES Implementation: Xiao Lai [35] affine/non-affine version; Attack: [19]; Work
 151 Factor: at least 2^{49} .

152 The attacks listed above may require to know the internal data representation and sometimes this
 153 means to produce a significant reverse engineering effort. An improved AES implementation is given
 154 in [36]. This implementation is immune to attacks described in [16,18] but it is not to the one presented
 155 in [37].

156 The first paper aiming to break all white-box implementations belonging to the framework
 157 introduced in [13] is [19], but it has the weak point to require some additional hypotheses. Differently,
 158 [38] breaks all the papers in Chow's framework by solving the affine equivalence problem (see [39]
 159 and [40]). Chow's framework has also been used by [41] and subsequently attacked by [42].

160 A significant advance from the attacker's point of view became feasible by shifting the focus
 161 from the attacks previously described to side channel attacks [43]. In particular, new approaches to
 162 verify the security of a white-box implementation have been proposed in [44] where Bos et al. present

163 differential fault analysis (DFA) and differential computational analysis (DCA) attacks¹. In addition,
 164 [47] and [48] explained more formally why DCA is effective against linear and nibble encoding, [43]
 165 provides an extensive analysis on the effectiveness of DCA, and [49] gives a general protection method
 166 for white-box implementations against DCA.

167 Obfuscation techniques or the randomization of the location of the lookup tables can be used to
 168 enhance security of white-box algorithms [50], while [51] examines how these techniques are successful
 169 against both DCA and differential power attacks (DPA). The paper [52] exploits noncommutative
 170 groups to obfuscate operation that should be made on commutative ones and it is employed in the IoT
 171 framework. Finally, an evaluation on software protections to white-box implementations is provided
 172 by [51].

173 Some improvements to DCA have been developed by [53] and [43]. The first one extends DCA to
 174 successfully address implementations using masking and shuffling techniques [53]. The second one
 175 provide a DCA-like collision attack with a good complexity [43].

176 Some paper such as [54], [55] and [56] address the problem of incompressibility or code hardness.
 177 The idea is that an attacker in the white-box framework should not be able to rewrite the code of
 178 some implementation in order to decrease the code-hardness. In [54] two incompressible white-box
 179 schemes called “WhiteKey” and “WhiteBlock” are introduced and one instance for each scheme
 180 is provided (called PuppyCipher and CoureurDesBois respectively), [55] describes the concept of
 181 code-hardness, time-hardness and memory-hardness, while [56] provides a new incompressible
 182 white-box implementation based on the assumption of one-way permutations.

183 We conclude our extensive analysis of implementations and attacks, citing a white-box signature
 184 scheme [57] and the methods [58] used to attack the most resistant implementation submitted to the
 185 white-box competition called “CHES 2017 CTF Challenge”.

186 In the sequel, we will analyze in detail two family of white-box cipher called SPACE (Section 4)
 187 and SPNbox (Section 5).

188 4. SPACE: a block cipher

189 SPACE is a block cipher developed by Bogdanov and Isobe in [23], that is based on a Feistel
 190 network. This cipher is designed so that security against key extraction in the white-box context
 191 reduces to the well studied problem of key recovery for block ciphers in the standard black-box setting.

192 SPACE is a generalized Feistel network [29]. Given a message
 193 $m \in \mathbb{F}^n$ and a secret key $k \in \mathcal{K}$, it encrypts m to a ciphertext $c \in \mathbb{F}^n$. In describing SPACE,
 194 three quantities are often employed: $n, n_a, n_b \in \mathbb{N}$. In particular, in [23] $n = 128, n_a \in \{8, 16, 24, 32\}$
 195 and $n_b = n - n_a$.

196 We summarize here the encryption procedure:

1. The state X^r at round r can be seen as given by $l = n/n_a$ vectors $x_i^r \in \mathbb{F}^{n_a}$ so

$$X^r = \{x_0^r, x_1^r, \dots, x_{l-1}^r\}.$$

- 197 2. $X^0 = m$, so it is initialized with the plaintext.
3. For $r \in \{1, \dots, R + 1\}$ the state is updated this way:

$$X^{r+1} = (F_{n_a}^r(x_0^r) \oplus (x_1^r || x_2^r || \dots || x_{l-1}^r)) || x_0^r$$

198 where $F_{n_a}^r : \mathbb{F}^{n_a} \rightarrow \mathbb{F}^{n_b}$ is the Feistel function and $||$ is the concatenation.

- 199 4. $X^{R+1} = c$ so we have found the ciphertext.

¹ Further information on fault-injection and differential power analysis attacks can be found in [45] and [46] respectively.

200 At each encryption round, the Feistel function takes x_0^r as input. Then $F_{n_a}^r(x_0^r)$ is added to the rest
 201 of the state $(x_1^r || \dots || x_{l-1}^r)$. The first n_b bits of the new state are given by the result of this operation.
 202 The last n_a are filled with x_0^r .

203 Now, consider π_t be the projection of Definition 2 and the Feistel function $F_{n_a}^r$ used by SPACE,
 204 specified in Definition 4.

Definition 4. Let ϕ_k be a block cipher and r the round number represented in binary with n_b digits (so we see it as an element of \mathbb{F}^{n_b}). The Feistel function $F_{n_a}^r$ is defined as

$$F_{n_a}^r(x) : \mathbb{F}^{n_a} \rightarrow \mathbb{F}^{n_b}$$

$$x \mapsto (\pi_{n_b}(\phi_k(\overbrace{0, \dots, 0}^{n_b} || x))) \oplus r.$$

205 We give a specific notation for the round independent part of F_{n_a} .

Definition 5. The round independent part of the Feistel function F_{n_a} is

$$F'_{n_a} : \mathbb{F}^{n_a} \rightarrow \mathbb{F}^{n_b}$$

$$x \mapsto \pi_{n_b}(\phi_k(\overbrace{0, \dots, 0}^{n_b} || x))$$

Notice that, differently from traditional Feistel networks, SPACE does not use round keys. There is one secret key k used by ϕ_k . This secret key cannot be hardcoded, hence F'_{n_a} is implemented as a look-up table. The reader might ask himself the reason for designing SPACE over another block cipher ϕ_k when ϕ_k could be directly implemented as a look-up table. It turns out that this second possibility cannot be developed. If we were to implement ϕ_k as a look-up table we would need $2^n \cdot n$ bits of space:

$$\begin{array}{l} \overbrace{(0, \dots, 0, 0)}^n \mapsto \overbrace{\phi_k(0, \dots, 0, 0)}^n \\ \overbrace{(0, \dots, 0, 1)}^n \mapsto \overbrace{\phi_k(0, \dots, 0, 1)}^n \\ \vdots \\ \overbrace{(1, \dots, 1, 1)}^n \mapsto \overbrace{\phi_k(1, \dots, 1, 1)}^n \end{array}$$

206 For $n = 128$ the construction of such a look-up table is practically impossible. Therefore Bogdanov
 207 and Isobe propose to truncate the output of ϕ_k , computed over a smaller domain:

$$\begin{array}{l} \overbrace{(0, \dots, 0)}^{n_b} || \overbrace{(0, \dots, 0, 0)}^{n_a} \mapsto \overbrace{\pi_{n_b}(\phi_k(0, \dots, 0 || 0, \dots, 0, 0))}^{n_b} \\ \overbrace{(0, \dots, 0)}^{n_b} || \overbrace{(0, \dots, 0, 1)}^{n_a} \mapsto \overbrace{\pi_{n_b}(\phi_k(0, \dots, 0 || 0, \dots, 0, 1))}^{n_b} \\ \vdots \\ \overbrace{(0, \dots, 0)}^{n_b} || \overbrace{(1, \dots, 1, 1)}^{n_a} \mapsto \overbrace{\pi_{n_b}(\phi_k(0, \dots, 0 || 1, \dots, 1, 1))}^{n_b} \end{array}$$

Figure 2. The value of each image of $F'_{n_a}(x)$ is saved as a row in a look-up table. Every row is indexed by the value of x , $x \in \{0, \dots, 2^{n_a} - 1\}$.

208 Since the first n_b zeros are used as padding in order to form an n -bit input to provide to ϕ_k , it is
 209 completely useless to store them, hence the look-up table implementation needs $2^{n_a} \cdot n_b$ bits. Thus, the
 210 size of the tables for different values of $n_a \in \{8, 16, 24, 32\}$ — SPACE(n_a, R), where R is the suggested
 211 number of rounds — is the following:

- 212 • SPACE-(8,300); Table: 3.84 KB
- 213 • SPACE-(16,128); Table: 918 KB
- 214 • SPACE-(24,128); Table: 218 MB

- SPACE-(32,128); Table: 51.5 GB

Notice that (1) AES white-box implementations of Chow et al. [13] and Xiao Lai [35] has a table of 752 KB and 20.5 MB respectively; (2) not all n_a values are suitable, indeed, for $n_a = 32$ and $n_a = 24$ the size of the table is not good enough to be used in practice. On the contrary, for $n_a = 16$ the table has the same size of that described in [13].

5. The SPNbox Family

The SPACE family of space-hard block ciphers [23] benefits of the Feistel structure from a security point of view and prevents the use of parallel execution (see Section 4). However, as suggested in [24], using an SPN-type design it is possible to satisfy the requirement of parallelism maintaining a suitably high level of space hardness. Thus, Bogdanov et al. described the SPNbox family of space-hard block ciphers [24]. Let us briefly explain their idea.

SPNbox- n_{in} is a substitution-permutation network (SPN) with a block length of n bits, a k -bit secret key, and based on n_{in} -bit substitution boxes.

State:

The state of SPNbox- n_{in} is representable as a vector of $t = n/n_{in}$ elements of n_{in} bits each:

$$X = \{X_0, \dots, X_{t-1}\}$$

Key Schedule:

The k -bit master key is expanded, $k_0, \dots, k_{R_{n_{in}}}$ round keys of n_{in} bits, by means of a Key Derivation Function (KDF) — e.g., PBKDF2 [59–62], ARGON2 [63], Scrypt [64], and so on:

$$(k_0, \dots, k_{R_{n_{in}}}) = KDF(k, n_{in} \cdot (R_{n_{in}} + 1))$$

Round Transformation:

We encrypt a plaintext X^0 and we get a ciphertext X^R , by using the following R transformations — e.g., $R = 10$:

$$X^R = (\bigcirc_{r=1}^R (\sigma^r \circ \theta \circ \gamma))(X^0)$$

The nonlinear layer γ is a substitution layer where t identical bijective n_{in} -bit S-boxes depending on the key are applied to the state:

$$\begin{aligned} \gamma : \mathbb{F}(2^{n_{in}})^t &\rightarrow \mathbb{F}(2^{n_{in}})^t \\ (X_0, \dots, X_{t-1}) &\mapsto (S_{n_{in}}(X_0), \dots, S_{n_{in}}(X_{t-1})) \end{aligned} \quad (3)$$

231

These identical S-boxes are constituted by an internal small block cipher of block length n_{in} bit.

232

The linear layer θ , a diffusion layer, applies a $t \times t$ MDS matrix to the state:

$$\begin{aligned} \theta : \mathbb{F}(2^{n_{in}})^t &\rightarrow \mathbb{F}(2^{n_{in}})^t \\ (X_0, \dots, X_{t-1}) &\mapsto (X_0, \dots, X_{t-1}) \cdot M_{n_{in}} \end{aligned}$$

233

234

235

236

The affine layer σ^r takes the state and adds round-dependent constants to it:

$$\sigma^r : \mathbb{F}(2^{n_{in}})^t \rightarrow \mathbb{F}(2^{n_{in}})^t$$

$$(X_0, \dots, X_{t-1}) \mapsto (X_0 \oplus C_0^r, \dots, X_{t-1} \oplus C_{t-1}^r),$$

237 with $C_i^r = (r-1) \cdot t + i + 1$ for $0 \leq i \leq t-1$.

238 The Underlying Small Block Ciphers:

The identical n_{in} -bit S-boxes in the γ layer (which depend on the key) are block ciphers. They are based on the round transformation of AES and they are formed by $R_{n_{in}}$ rounds operating on a state $x = \{x_0, \dots, x_{l-1}\}$ of l bytes, where $l = n_{in}/8$:

$$S_{n_{in}} : \mathbb{F}(2^8)^l \rightarrow \mathbb{F}(2^8)^l$$

$$x \mapsto (\bigcirc_{i=1}^{R_{n_{in}}} (AK^i \circ MC_{n_{in}} \circ SB))(AK^0(x))$$

239 where SB, MC and AK indicate the AES transformations SubBytes, MixColumns and AddRoundKey,
 240 respectively. Notice that (a) the number of rounds $R_{n_{in}}$ that [24] suggests are $R_{32}=16$, $R_{24}=20$, $R_{16}=32$
 241 and $R_8=64$; (b) different matrices are employed in the $MC_{n_{in}}$ round transformation. More precisely, for
 242 $n_{in}=32$ we use the MC matrix of AES, while in the other cases a sub-matrix of MC is used. If $n_{in}=8$,
 243 $MC_{n_{in}}$ is the identity map's matrix. Note that, as for the Feistel function in SPACE, in the white-box
 244 setting the small block ciphers $S_{n_{in}}$ are implemented as lookup tables.

245 6. Issues and possible solutions

246 Although the white-box implementation of the cipher is very important, it may have some
 247 limitations due to the key embedded into the device. If several devices have to communicate with a
 248 server and such devices do not support TLS due to insufficient resources, the server needs to manage
 249 a number of keys (pre-shared or not) in order to decrypt the messages. In a white-box context this
 250 means having a number of different implementations that run on our server and this is not a good
 251 idea. Therefore, the server will be provided with a fast black-box implementation of the cipher.

252 Figure 3 helps us to visualize this idea, where a white-box implementation runs on a number of
 253 devices and a fast black-box implementation runs on our server.

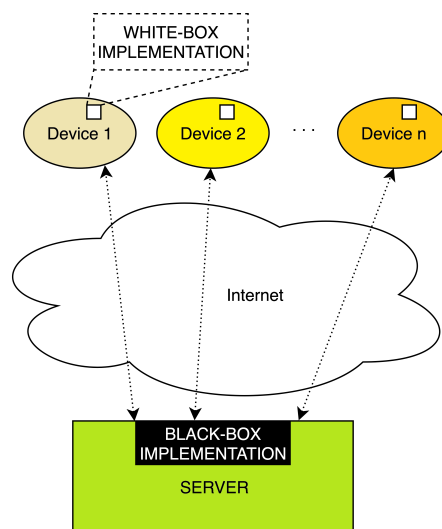


Figure 3. A black-box implementation (server-side)

254 In order to design a fast black-box implementation of a white-box cipher, we modify the inner
 255 round described in Section 5, increasing the number of bits of the key used in each round. In particular,
 256 we replace the AES' ShiftRow transformation, omitted by [24], with a key-dependent circular bit shift
 257 transformation (see Figures 4 and 5).

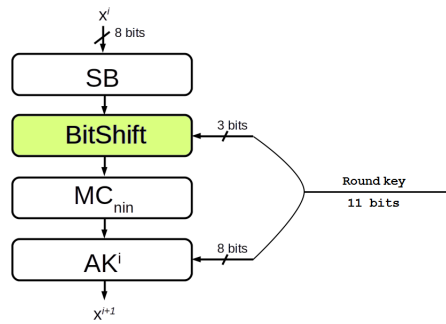


Figure 4. A BitShift key-dependent: Increasing the size of the round key from 8 to 11 bits.

258 If we are shifting 8 bits of the state, i.e., $n_{in}=8$, 3 bits are required to execute the circular shift. Thus,
 259 we use 11 bits of the key in each round i : 8 of them for the AK^i transformation and 3 for the BitShift
 260 transformation. If the state doubled, tripled, or quadrupled, i.e., $n_{in}=16, 24, 32$, the bits of the key used
 261 are $11 \times 2 = 22$, $11 \times 3 = 33$ and $11 \times 4 = 44$ respectively.

262 Notice that the implementation of [24] employs the AES-NI instructions, while the idea described
 263 in this paper does not. In the encryption phase ($n_{in}=32, 24, 16$), the matrices involved in the computation
 264 of the MixColumns transformation (A_{24} , and A_{16} for short) are sub-matrices of that used in AES (A_{32}).
 265 On the contrary, in the decryption phase, we need to invert A_{24} and A_{16} . Since their inverse matrices
 266 are not sub-matrices of A_{32}^{-1} and the decryption instruction of AES-NI is based only on A_{32}^{-1} , for
 267 $n_{in}=24, 16$ we cannot use the AES-NI instructions. Anyway, in IoT context, the impossibility of using
 268 AES-NI instructions is not a problem in itself because not all IoT devices support this instruction set.

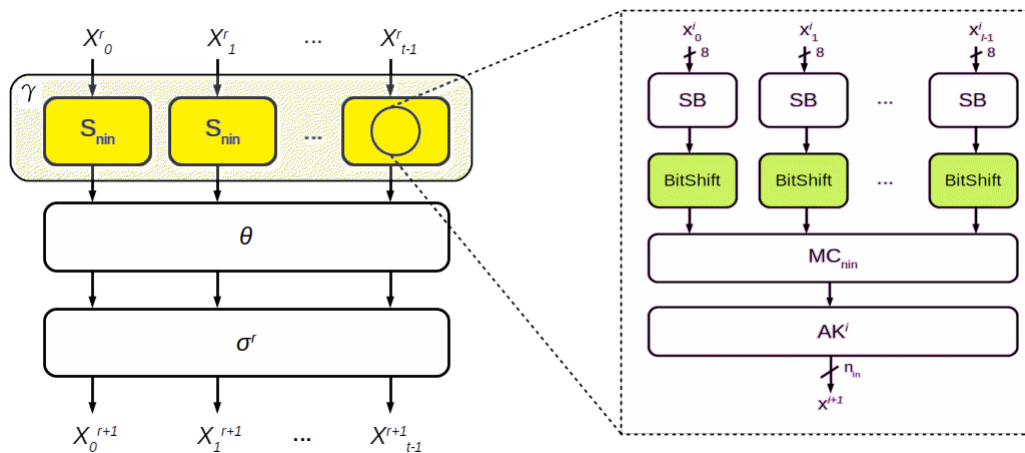


Figure 5. SPNbox: a new inner round γ

269 7. Testing activities

270 The testing activity reported is twofold. In the first part, we measure the performance of internal
 271 layer γ (see Algorithm 1) — the external part (layer θ and σ) is exactly the same as in [24], so it would
 272 be pointless to evaluate it.

273 In the second part, as explained in Section 6, we examine the cipher in the IoT context, where
 274 black-box and white-box implementations are involved.

275 7.1. 32/64-bit architectures

276 We compared the performance of internal layer γ (yellow rectangles of Figure 5) with and without
 277 BitShift transformation (green rectangles of Figure 5) for different n_{in} sizes. We avoid the operations
 278 involved in θ and σ layers.

Algorithm 1: Layer γ with BitShift transformation

```

1 Function SPNbox(state):
2   for  $r = 1 \rightarrow R$  do
3     layer_gamma(state)
4     layer_theta(state)
5     layer_sigma(state, r)
6 Function layer_gamma(state):
7   Set  $n_{in} = 8, 16,$  or  $32$ 
8   foreach chunk of length  $n_{in}$  in state do
9      $S_{n_{in}}$ (state)
10 Function  $S_{n_{in}}$ (state):
11   AddRoundKey(state)
12   for  $i = 1 \rightarrow R_{n_{in}}$  do
13     SubBytes(state)
14     BitShift(state)
15     MixColumns(state)
16     AddRoundKey(state)
17 Function layer_theta(state):
18   return
19 Function layer_sigma(state,r):
20   return

```

279 We run our code on laptops with different hardware configurations. More precisely, our laptops
280 are equipped with

- 281 • Intel® Core™ i3-330M, 2.13 GHz processor with 3 MB SmartCache, 8 GB RAM and Ubuntu
282 18.04.1 LTS 64-bit. The source code has been compiled with GCC 7.3.0 with -O3 optimization
283 enabled (see Table 1);
- 284 • Intel® Core™ i3-350M, 2.26 GHz processor with 3 MB SmartCache, 8 GB RAM and Ubuntu
285 18.04.2 LTS 64-bit. The source code has been compiled with GCC 7.4.0 with -O3 optimization
286 enabled (see Table 2);
- 287 • Intel® Core™ i7-2860QM, 2.50/3.60 GHz processor with 8 MB SmartCache, 16 GB RAM and
288 Kubuntu 18.10 64-bit. The source code has been compiled with GCC 7.3.0 with -O3 optimization
289 enabled (see Table 3);
- 290 • Intel® Core™ i7-5500U, 2.40/3.00 GHz processor with 4 MB Cache, 8 GB RAM and Ubuntu
291 18.04.2 LTS 64-bit. The source code has been compiled with GCC 7.4.0 with -O3 optimization
292 enabled (see Table 4);
- 293 • Intel® Core™ i7-8550U CPU, 1.80/4.00 GHz processor with 8 MB SmartCache, 32 GB RAM
294 and Ubuntu 18.04.2 LTS 64-bit. The source code has been compiled with GCC 7.4.0 with -O3
295 optimization enabled (see Table 5);
- 296 • Intel® Core™ i3-350M, 2.26 GHz processor with 3 MB SmartCache, 4 GB RAM and Debian
297 GNU/Linux 9 32-bit. The source code has been compiled with GCC 6.3.0 with -O3 optimization
298 enabled (see Table 6);

299 Tables 1, 2, 3, 4, 5, 6 show the time required to encrypt/decrypt one million of different plaintexts (fixed
300 size of 128 bits) using the same key (randomly chosen). Notice that in addition to the key bits needed
301 for the initial AddRoundKey AK^0 , SPNbox layer γ uses 512 key bits — i.e. 512 bit = 16 round \times 32 bit
302 ($n_{in}=32$), or 512 bit = 32 round \times 16 bit ($n_{in}=16$), or 512 bit = 64 round \times 8 bit ($n_{in}=8$). Therefore, we
303 set to 512 the minimum amount of key bits to be used in our solution. In particular, we will execute:
304 12 rounds ($R_{n_{in}}=12$), using 528 key bits ($n_{in}=32$); 24 rounds ($R_{n_{in}}=24$), using 528 key bits ($n_{in}=16$); and
305 finally 47 rounds ($R_{n_{in}}=47$), using 517 key bits ($n_{in}=8$).

Table 1. results of tests on i3-330M with Ubuntu 18.04.1 LTS 64-bit.

| | γ | γ with BitShift |
|--------------------------|------------|------------------------|
| $n_{in}=32$, encryption | 1.178316 s | 0.955048 s |
| $n_{in}=32$, decryption | 1.447580 s | 1.168507 s |
| $n_{in}=16$, encryption | 3.946748 s | 3.222751 s |
| $n_{in}=16$, decryption | 4.193261 s | 3.308678 s |
| $n_{in}=8$, encryption | 2.547156 s | 2.192452 s |
| $n_{in}=8$, decryption | 2.564750 s | 2.250102 s |

Table 2. results of tests on i3-350M with Ubuntu 18.04.2 LTS 64-bit.

| | γ | γ with BitShift |
|--------------------------|------------|------------------------|
| $n_{in}=32$, encryption | 1.116117 s | 0.902140 s |
| $n_{in}=32$, decryption | 1.367435 s | 1.150235 s |
| $n_{in}=16$, encryption | 3.717744 s | 3.035942 s |
| $n_{in}=16$, decryption | 3.954781 s | 3.116000 s |
| $n_{in}=8$, encryption | 2.395998 s | 2.061877 s |
| $n_{in}=8$, decryption | 2.405397 s | 2.114405 s |

Table 3. results of tests on i7-2860QM with Kubuntu 18.10 64-bit.

| | γ | γ with BitShift |
|--------------------------|------------|------------------------|
| $n_{in}=32$, encryption | 0.837671 s | 0.668838 s |
| $n_{in}=32$, decryption | 0.925293 s | 0.816856 s |
| $n_{in}=16$, encryption | 2.667934 s | 2.147471 s |
| $n_{in}=16$, decryption | 2.811657 s | 2.394600 s |
| $n_{in}=8$, encryption | 1.886357 s | 1.565764 s |
| $n_{in}=8$, decryption | 2.030491 s | 1.777118 s |

Table 4. results of tests on i7-5500U with Ubuntu 18.04.2 LTS 64-bit.

| | γ | γ with BitShift |
|--------------------------|------------|------------------------|
| $n_{in}=32$, encryption | 0.861415 s | 0.701899 s |
| $n_{in}=32$, decryption | 0.954985 s | 0.782088 s |
| $n_{in}=16$, encryption | 2.980274 s | 2.461575 s |
| $n_{in}=16$, decryption | 3.155612 s | 2.543056 s |
| $n_{in}=8$, encryption | 1.860916 s | 1.774127 s |
| $n_{in}=8$, decryption | 1.879749 s | 1.785562 s |

Table 5. results of tests on i7-8550U with Ubuntu 18.04.2 LTS 64-bit.

| | γ | γ with BitShift |
|--------------------------|------------|------------------------|
| $n_{in}=32$, encryption | 0.681576 s | 0.526522 s |
| $n_{in}=32$, decryption | 0.723118 s | 0.587942 s |
| $n_{in}=16$, encryption | 2.396308 s | 1.898987 s |
| $n_{in}=16$, decryption | 2.462049 s | 1.933232 s |
| $n_{in}=8$, encryption | 1.160104 s | 1.258072 s |
| $n_{in}=8$, decryption | 1.179036 s | 1.248327 s |

Table 6. results of tests on i3-350M with Debian GNU/Linux 9 32-bit.

| | γ | γ with BitShift |
|--------------------------|------------|------------------------|
| $n_{in}=32$, encryption | 1.247818 s | 1.041543 s |
| $n_{in}=32$, decryption | 1.967226 s | 1.558086 s |
| $n_{in}=16$, encryption | 3.721377 s | 3.381363 s |
| $n_{in}=16$, decryption | 4.164744 s | 3.262065 s |
| $n_{in}=8$, encryption | 2.399780 s | 2.065451 s |
| $n_{in}=8$, decryption | 2.412146 s | 2.127425 s |

306 Our testing activities show that implementations with BitShift are generally faster than those
 307 without it. In particular, several cases show that the improvement in the execution time exceeds 20%.
 308 Only in Table 5, $n_{in}=8$, encryption and decryption, we find a different result.

Algorithm 2: MQTT: testing activity executed for each payload (16, 64, 128, and 1024 bytes)

```

1 Function layer_gamma_without_Bitshift(state,  $n_{in}$ , key):
2   foreach chunk of length  $n_{in}$  in state do
3     AddRoundKey(state, key)
4     for  $i = 1 \rightarrow R_{n_{in}}$  do
5       SubBytes(state)
6       MixColumns(state)
7       AddRoundKey(state, key)

8 Function layer_gamma_with_Bitshift(state,  $n_{in}$ , key):
9   foreach chunk of length  $n_{in}$  in state do
10    AddRoundKey(state, key)
11    for  $i = 1 \rightarrow R_{n_{in}}$  do
12      SubBytes(state)
13      BitShift(state)
14      MixColumns(state)
15      AddRoundKey(state, key)

16 Function main():
17   Open a connection
18   Set key  $k = \text{Random}()$ 
19   Set plaintext  $p = \text{Random}()$ 
20   foreach  $n_{in}$  in (8, 16, 32) do
21     Set timer  $t_1 = 0$ 
22     Set  $p_1 = p$ 
23     for  $i = 1 \rightarrow 100$  do
24       for  $j = 1 \rightarrow 10,000$  do
25         layer_gamma_without_BitShift( $p_1$ ,  $n_{in}$ ,  $k$ )
26       Send  $p_1$  as payload with a MQTT message
27     Stop timer  $t_1$ 
28     Set timer  $t_2 = 0$ 
29     Set  $p_2 = p$ 
30     for  $i = 1 \rightarrow 100$  do
31       for  $j = 1 \rightarrow 10,000$  do
32         layer_gamma_with_BitShift( $p_2$ ,  $n_{in}$ ,  $k$ )
33       Send  $p_2$  as payload with a MQTT message
34     Stop timer  $t_2$ 
35     Compare  $t_1$  and  $t_2$ 
36     Close the connection

```

309 7.2. IoT environment

310 The testing activity has been performed using MQTT [65], a lightweight communication protocol
311 designed for small sensors and mobile devices in low bandwidth environments. By default data are
312 sent in clear text over the Internet, thus we encrypt data contained in the payload. We measure the
313 performance of layer γ as described in Algorithm 2. More precisely, we compare the performances
314 with and without BitShift transformation for different n_{in} — size of 32, 16, and 8 bits — encrypting
315 one million of different plaintexts — size of 16, 64, 256, and 1024 bytes — using the same key. Then,
316 we send one hundred MQTT messages, each of which contains 10,000 encrypted payloads. Finally,
317 adopting the same approach, the server collects and decrypts the same number of MQTT messages
318 with encrypted payloads.

Table 7. Encryption/decryption operations with a black-box implementation (server-side)

| Payload (Bytes) | n_{in} (Bits) | Encryption | | | Decryption | | |
|--------------------|--------------------|--------------|---------------|---------|--------------|---------------|---------|
| | | w/o BitShift | with BitShift | Gain | w/o BitShift | with BitShift | Gain |
| 16 | 32 | 3.668s | 3.319s | 9.507% | 0.893s | 0.741s | 16.999% |
| | 16 | 6.335s | 5.763s | 9.037% | 3.096s | 2.412s | 22.091% |
| | 8 | 4.510s | 4.882s | -8.254% | 1.479s | 1.551s | -4.929% |
| 64 | 32 | 6.679s | 5.601s | 16.139% | 3.636s | 2.950s | 18.865% |
| | 16 | 14.869s | 12.362s | 16.860% | 12.488s | 10.023s | 19.739% |
| | 8 | 8.817s | 9.616s | -9.060% | 6.183s | 6.446s | -4.253% |
| 128 | 32 | 16.021s | 13.847s | 13.569% | 14.166s | 11.827s | 16.512% |
| | 16 | 51.098s | 38.998s | 23.680% | 50.632s | 39.596s | 21.798% |
| | 8 | 24.280s | 25.709s | -5.884% | 24.454s | 25.825s | -5.607% |
| 1024 | 32 | 54.047s | 41.716s | 22.816% | 56.494s | 47.065s | 16.690% |
| | 16 | 191.262s | 151.101s | 20.998% | 195.424s | 154.029s | 21.182% |
| | 8 | 92.651s | 98.998s | -6.850% | 93.744s | 98.362s | -4.926% |

319 Our testing activity has been executed on a machine equipped with an Intel® Core™ i7-6500U
 320 CPU @ 2.50GHz x 4 processor, with 12 GB SDRAM DDR4-2133, Intel® HD Graphics 520 (Skylake
 321 GT2) GPU and operating system Ubuntu 18.04.2 TLS. We used *Mosquitto* [66] version 1.4.15, which
 322 implements the MQTT protocol versions 3.1.1. The source code has been compiled with GCC 7.4.0,
 323 -O3 optimization enabled. Table 7 summarizes the results obtained.

324 In particular, for the encryption phase, we got a highest gain (23.680%) in the case of 128-byte
 325 payload and $n_{in} = 16$, while the highest loss (−9.060%) in the case of a 64-byte payload and $n_{in} = 8$.
 326 For the decrypt phase, the highest gain (22.091%) is obtained with a 16-byte payload and $n_{in} = 16$, and
 327 the highest loss (−5.607%) with a 128-byte payload and $n_{in} = 8$. Notice that the case $n_{in} = 8$ turned
 328 out to be the worst one.

329 8. Conclusions

330 In the era of Internet of Things the involved devices are usually lightweight, so they cannot
 331 perform heavy computations nor store a huge amount of data. In addition, these data might be
 332 sensitive — energy consumptions, medical records, and so on — and could be sent in an unprotected
 333 environment. In a white-box scenario, an attacker could easily read these data because she/he has full
 334 access to the whole execution platform and white-box cryptography can be used to secure data in this
 335 specific context.

336 Considering the effectiveness of side-channel attacks, new ciphers has been designed with
 337 white-box attack model in mind. In this paper, we focused on the SPNbox family [24], suggesting
 338 how to increase the number of key bits used in each round and showing that this improvement affects
 339 the performance of the cipher. The introduction of a key-dependent circular bit shift transformation
 340 helped us to increase the keyspace and to reduce the number of rounds of the cipher, reducing the
 341 execution time too.

342 We described and analyzed the performance of the modified cipher in the IoT context, where both
 343 white-box and black-box implementations may be required. In particular, we measured its performance
 344 (a) on 32/64-bit architectures and (b) encrypting the payload of an IoT messaging protocol. Our testing
 345 activities have been executed on consumer laptops. The results obtained encrypting and decrypting
 346 one million of different 128-bit plaintexts on 32/64-bit architectures showed that the execution time for
 347 layer γ is reduced up to 22% while the highest loss is about 8%.

Moreover, the testing activities performed with lightweight protocol MQTT got a gain of about 23% and 22% (encryption and decryption phase, respectively) while a loss of about 9% and 5%. In all our testing activities the case $n_{in} = 8$ turns out to be the worst one.

Possible future works are try to (a) understand in details why current implementation fails for $n_{in} = 8$ and (b) implement a communication protocol based on TLS-PSK, in order to compare the performance of white-box implementations with those of lightweight ciphers.

Author Contributions: All the authors contributed equally to the work. D.G.V.A., F.C., and A.S. wrote the code and executed testing activities; M.C., N.F., and A.V. wrote the manuscript; All the authors discussed the results and provided critical comments; A.V. supervised the testing activities.

Conflicts of Interest: The authors declare no conflict of interest.

References

- Ashton, K. That ‘internet of things’ thing. *RFID journal* **2009**, *22.7*, 97–114.
- Harini, S.; Jothika, K.; Jayashree, K. A Survey on Privacy and Security in Internet of Things. *Int. Journ. of Innov. in Engin. and Tech.* **2017**, *8*, 129–134.
- Bertino, E. Data Security and Privacy in the IoT. *EDBT* **2016**, *2016*, 1–3.
- Tsai, C.; Lai, C.F.; Chiang, M.C.; Yang, L.T. Data mining for internet of things: A survey. *IEEE Comm. Surv. & Tut.* **2013**, *16.1*, 77–97.
- Schlesinger, M.; Parisi, D. The agent-based approach: A new direction for computational models of development. *Dev. Rev.* **2001**, *21.1*, 121–146.
- Visconti, A.; Tahayori, H. Artificial immune system based on interval type-2 fuzzy set paradigm. *Appl. Soft Comput.* **2011**, *11.6*, 4055–4063.
- Lee, S.; Kyon-Mo, Y.; Sung-Bae, C. Integrated modular Bayesian networks with selective inference for context-aware decision making. *Neurocomp.* **2015**, *163*, 38–46.
- Visconti, A.; Tahayori, H. Detecting misbehaving nodes in MANET with an artificial immune system based on type-2 fuzzy sets. In *International Conference for Internet Technology and Secured Transactions*, Proceedings of the IEEE 4th International Conference for Internet Technology and Secured Transactions 2009, London, UK, 9 - 13 November 2009; IEEE.
- Shi, Y.; Wei, W.; He, Z.; Fan, H. An ultra-lightweight white-box encryption scheme for securing resource-constrained IoT devices. In Proceedings of the 32nd Annual Conference on Computer Security Applications, Los Angeles, California, USA, 5 - 8 December 2016; ACM: New York, USA, 2016.
- Shamir, A.; Van Someren, N. Playing “hide and seek” with stored keys. In Proceedings of the conference Financial Crypto 1999 (FC’99), Anguilla, BWI, 22 - 25 February 1999; Franklin M., Ed.; Springer: Heidelberg, Germany; pp. 118–124.
- Boneh, D.; DeMillo, R.A.; Lipton, R.J. On the importance of checking cryptographic protocols for faults (extended abstract). In Proceedings of the conference EUROCRYPT97, Konstanz, Germany, 11-15 May 1997; Fumy W., Ed.; Springer: Heidelberg, Germany; pp. 37–51.
- Biham, E.; Shamir, A. Differential fault analysis of secret key cryptosystems. In Proceedings of the conference CRYPTO97, Santa Barbara, California, USA, 17 - 21 August 1997; Kaliski B.S., Ed.; Springer: Heidelberg, Germany; pp. 513–525.
- Chow, S.; Eisen, P.; Johnson, H.; Van Oorschot, P.C. White-box cryptography and an AES implementation. In Proceedings of the International Workshop on Selected Areas in Cryptography 2002, John’s, Newfoundland, Canada, 15 - 16 August 2002; Nyberg K., Heys H., Eds.; Springer: Berlin, Germany; pp. 250–270.
- Cho, J.; Kyu Young, C.; Dukjae M. Hybrid WBC: Secure and efficient encryption schemes using the White-Box Cryptography. *IACR Cryptol. ePrint archive* **2015**, *2015*, 800.
- Chow, S.; Eisen, P.; Johnson, H.; Van Oorschot, P.C. A white-box DES implementation for DRM applications. In Proceedings of the ACM Workshop on Digital Rights Management, Washington, DC, USA, 18 November 2002; Feigenbaum J., Ed.; Springer: Berlin, Germany; pp. 1–15.
- Billet, O.; Henri, G.; Charaf, E. Cryptanalysis of a white box AES implementation. In Proceedings of the International Workshop on Selected Areas in Cryptography, Waterloo, Canada, 9 - 10 August 2004; Handschuh H., Hasan M.A., Eds.; Springer: Berlin, Germany; pp. 227–240.

- 398 17. De Mulder, Y.; Roelse, P.; Preneel, B. Revisiting the BGE attack on a white-box AES implementation. *IACR*
399 *Cryptol. ePrint archive* **2017**, 2013, 450.
- 400 18. De Mulder, Y.; Roelse, P.; Preneel, B. Cryptanalysis of the Xiao–Lai white-box AES implementation. In
401 Proceedings of the International Conference on Selected Areas in Cryptography 2012, Windsor, ON, Canada,
402 15 - 16 August 2012; Knudsen L.R., Wu H., Eds.; Springer: Berlin, Germany; pp. 34–39.
- 403 19. Michiels, W.; Gorissen, P.; Hollmann, H.D.L. Cryptanalysis of a generic class of white-box implementations.
404 In Proceedings of the International Workshop on Selected Areas in Cryptography 2008, Sackville, New
405 Brunswick, Canada, 14 - 15 August 2008; Avanzi R.M., Keliher L., Sica F., Eds.; Springer: Berlin, Germany; pp.
406 414–428.
- 407 20. Lepoint, T.; Rivain, M.; De Mulder, Y.; Roelse, P.; Preneel, B. Two attacks on a white-box AES implementation.
408 In Proceedings of the International Conference on Selected Areas in Cryptography 2013, Burnaby, BC,
409 Canada, 14 - 16 August 2013; Lange T., Lauter K., Lisoněk P., Eds.; Springer: Berlin, Germany; pp. 265–285.
- 410 21. Jacob, M.; Boneh, D.; Felten, E. Attacking an obfuscated cipher by injecting faults. In Proceedings of the
411 ACM Workshop on Digital Rights Management, 2002. Washington, DC, USA, 18 November 2002; Springer:
412 Berlin, Germany; pp. 16–31.
- 413 22. Biryukov, A.; Bouillaguet, C.; Khovratovich, D. Cryptographic schemes based on the ASASA structure:
414 Black-box, white-box, and public-key (Extended Abstract). In *Advances in Cryptology*, Proceedings of
415 ASIACRYPT 2014, Kaohsiung, Taiwan, 7 - 11 December 2014; Sarkar, P., Iwata, T., Eds.; Springer: Berlin,
416 Germany, 2014; pp. 63–84.
- 417 23. Bogdanov, A.; Takanori, I. White-box cryptography revisited: space-hard ciphers. In Proceedings of the 22nd
418 ACM SIGSAC Conference on Computer and Communications Security, Denver, Colorado, USA, 12 - 16
419 October 2015; ACM: New York, NY, USA, 2015; pp. 1050–1069.
- 420 24. Bogdanov, A.; Takanori I.; Tischhauser, E. Towards practical whitebox cryptography: optimizing efficiency
421 and space hardness. In Proceedings of ASIACRYPT 2016, Hanoi, Viet Nam, 4 - 8 December 2016; Cheon J.H.,
422 Tsuyoshi T., Eds.; Springer: Berlin, Germany; pp. 126–158.
- 423 25. Shi, Y.; Wei, W.; Fan, H.; Au, M. H.; Luo, X. A Light-Weight White-Box Encryption Scheme for Securing
424 Distributed Embedded Devices. *IEEE Trans. on Comp.* in press.
- 425 26. Biryukov, A.; Shamir, A. Structural cryptanalysis of SASAS. *Journ. of crypt.* **2014**, *23.4*, 505–518.
- 426 27. Cioschi, F.; Fornari, N.; Visconti, A. White-Box Cryptography: A Time-Security Trade-Off for the SPNbox
427 Family. In Proceedings 2nd International Conference on Wireless Intelligent and Distributed Environment
428 for Communication (WIDECOM 2019), Milan, Italy, 11 - 13 February 2019; Woungang I., Dhurandher S.,
429 Eds.; Springer: Cham; pp. 153–166.
- 430 28. Shannon, C.E. Communication theory of secrecy systems. *Bell syst. tech. journ.* **1949**, *28.4*, 656–715.
- 431 29. Feistel, H. Cryptography and computer privacy. *Sci. amer.* **1973**, *228.5*, 15–23.
- 432 30. Lee, S.; Jho, N. S.; Kim, M. A Key Leakage Preventive White-box Cryptographic Implementation. *IACR*
433 *Cryptol. ePrint archive* **2018**, 2018, 1047.
- 434 31. Bringer, J.; Chabanne, H.; Dottax, E. Perturbing and protecting a traceable block cipher. In *Communications*
435 *and Multimedia Security*, Proceedings of the 10th IFIP TC-6 TC-11 International Conference, Heraklion, Crete,
436 Greece, 19-21 october 2006; Springer: Berlin, Heidelberg, Germany; pp. 109–119.
- 437 32. Bringer, J., Chabanne, H., Dottax, E. White box cryptography: Another attempt. *IACR Cryptol. ePrint archive*
438 **2006**, 2006, 468.
- 439 33. De Mulder, Y.; Wyseur, B.; Preneel, B. Cryptanalysis of a Perturbated White-Box AES Implementation. In
440 *Progress in Cryptology*, Proceedings of the conference INDOCRYPT 2010, Hyderabad, India, 12-15 December
441 2010; Gong G., Gupta K.C. Eds.; Springer: Berlin, Heidelberg, Germany; pp 292–310.
- 442 34. Karroumi, M. Protecting white-box AES with dual ciphers. In Proceedings of the International Conference
443 on Information Security and Cryptology 2010, Seoul, Korea, 1 - 3 December 2010; Rhee K.H., Nyang D., Eds.;
444 Springer: Berlin, Germany; pp. 278–291.
- 445 35. Xiao, Y.; Xuejia, L. A secure implementation of white-box AES. In Proceedings of the 2009 2nd International
446 Conference on Computer Science and its Applications, Jeju, Korea (South), 10 - 12 December 2009; IEEE:
447 2009; pp. 1–6.
- 448 36. Luo, R., Lai, X., You, R. A new attempt of white-box AES implementation, Proceedings of the International
449 Conference on Security, Pattern Analysis, and Cybernetics, Wuhan, China, 18-19 October 2014; IEEE; pp.
450 423–429.

- 451 37. Bai, K.; Wu, C.; Zhang, Z. Protect white-box AES to resist table composition attacks. *IET Information Security*,
452 **2018**, *12*(4), 305–313.
- 453 38. Derbez, P.; Fouque, P. A.; Lambin, B.; Minaud, B. On Recovering Affine Encodings in White-Box
454 Implementations. In Proceedings of the Conference on Cryptographic Hardware and Embedded Systems
455 2016 (CHES2016), Santa Barbara, USA, August 17–19 2016; Gierlichs B., Poschmann A.Y., Eds; Springer:
456 Heidelberg, Germany; pp. 121–149.
- 457 39. Biryukov, A.; De Cannière, C.; Braeken, A.; Preneel, B. A toolbox for cryptanalysis: Linear and affine
458 equivalence algorithms. In *Advances in Cryptology - EUROCRYPT 2003*, Proceedings of the International
459 Conference on the Theory and Applications of Cryptographic Techniques, Warsaw, Poland, 4–8 May 2003;
460 Springer: Berlin, Germany, Heidelberg; pp.33–50.
- 461 40. Dinu, I. An improved affine equivalence algorithm for random permutations. In *Advances in Cryptology* ,
462 Proceedings of the conference EUROCRYPT 2018, Tel Aviv, Israel, April 29 - May 3 2018; Springer: Cham,
463 Germany; pp. 413–442.
- 464 41. Xu, T.; Wu, C.; Liu, F.; Zhao, R. Protecting white-box cryptographic implementations with obfuscated round
465 boundaries. *Science China Information Sciences*, **2017**, *61*(3).
- 466 42. Yongjin, Y.; Dong-Chan, K.; Hun, B. C.; Junbum, S. Cryptanalysis of the Obfuscated Round Boundary
467 Technique for Whitebox Cryptography. *Science China Information Sciences*.
- 468 43. Rivain, M.; Wang, J. Analysis and Improvement of Differential Computation Attacks against
469 Internally-Encoded White-Box Implementations. *IACR Trans. on Crypt. Hardware and Embedded Systems*.
470 **2019**, 225–255.
- 471 44. Bos, J. W.; Hubain, C.; Michiels, W.; Teuwen, P. Differential computation analysis: Hiding your white-box
472 designs is not enough. In Proceedings of the Conference on Cryptographic Hardware and Embedded
473 Systems 2016 (CHES2016), Santa Barbara, USA, August 17–19 2016; Gierlichs B., Poschmann A.Y., Eds;
474 Springer: Heidelberg, Germany; pp. 215–236.
- 475 45. Dusart, P.; Letourneux, G.; Vivolo, O. Differential fault analysis on AES. In Proceedings of the International
476 Conference on Applied Cryptography and Network Security 2003, Kunming, China, 16 - 19 October 2003;
477 Zhou J., Moti Y., Han Y., Eds.; Springer: Berlin, Germany; pp. 293–306.
- 478 46. Kocher, P.; Jaffe, J.; Jun, B.; Rohatgi, P. Introduction to differential power analysis. *Journ. of Crypt. Engin.* **2011**,
479 *1.1.*, 5–27.
- 480 47. Alpirez Bock, E.; Bos, J.W.; Brzuska, C.; Hubain, C.; Michiels, W.; Mune, C.; Sanfeliu Gonzalez, E.; Teuwen, P.;
481 Treff, A. White-Box Cryptography: Don't Forget About Grey Box Attacks. *IACR Cryptol. ePrint archive* **2017**,
482 2017, 355.
- 483 48. Bock, E.A.; Brzuska, C.; Michiels, W.; Treff, A. On the ineffectiveness of internal encodings - revisiting the
484 DCA attack on white-box cryptography. In Proceedings of the 16th International Conference on Applied
485 Cryptography and Network Security (ACNS2018), Leuven, Belgium, 2–4 July 2018; Preenel B., Vercauteren
486 F., Eds.; Springer: Heidelberg, Germany; pp. 103–120.
- 487 49. Biryukov, A.; Udovenko, A. Attacks and countermeasures for white-box designs. In International Conference
488 on the Theory and Application of Cryptology and Information Security, Kobe, Japan, 8–12 December 2019;
489 Springer: Cham, Germany; pp. 373–402.
- 490 50. Lee, S.; Kim, T.; Kang, Y. A masked white-box cryptographic implementation for protecting against
491 differential computation analysis. *IEEE Transactions on Information Forensics and Security*, **2018**, *13*(10),
492 2602–2615.
- 493 51. Banik, S.; Bogdanov, A.; Isobe, T.; Jepsen, M. Analysis of software countermeasures for whitebox encryption.
494 *IACR Transactions on Symmetric Cryptology*, **2017**, 307–328.
- 495 52. Marin, L. White Box Implementations Using Non-Commutative Cryptography. *Sensors*, **2019**, *19*,5.
- 496 53. Bogdanov, A.; Rivain, M.; Vejre, P.S.; Wang, J. Higher-order DCA against standard side-channel
497 countermeasures. *IACR Cryptol. ePrint archive* **2018**, 2018, 869.
- 498 54. Fouque, P.A.; Karpman, P.; Kirchner, P.; Minaud, B. Efficient and provable white-box primitives. In *Advances*
499 *in Cryptology* , Proceedings of ASIACRYPT 2016, Hanoi, Viet Nam, 4 - 8 December 2016; Cheon J. H., Takagi
500 T. Eds.; Springer: Berlin, Heidelberg, 2016; pp 159 – 188
- 501 55. Biryukov, A.; Perrin, L. Symmetrically and Asymmetrically Hard Cryptography. Proceedings of the
502 International Conference on the Theory and Application of Cryptology and Information Security, Hong
503 Kong, China, 3 - 7 December 2017; Springer: Cham, Germany; pp. 417–445

- 504 56. Bock, E. A.; Amadori, A.; Bos, J. W.; Brzuska, C.; Michiels, W. Doubly half-injective PRGs for incompressible
505 white-box cryptography. In Cryptographers' Track at the RSA Conference, S. Francisco, California, USA, 4 -
506 8 March 2019; Springer, Cham, Germany; pp. 189-209.
- 507 57. Feng, Q.; He, D.; Wang, H.; Kumar, N.; Choo, K. K. R. White-Box Implementation of Shamir's Identity-Based
508 Signature Scheme. *IEEE Systems Journal*, **2019**.
- 509 58. Goubin, L.; Paillier, P.; Rivain, M.; Wang, J. How to reveal the secrets of an obscure white-box implementation.
510 *Journal of Cryptographic Engineering*, **2018**, 1-18.
- 511 59. Moriarty, K.; Kaliski, B.; Rusch, A. PKCS# 5: Password-Based Cryptography Specification Version 2.1. *Internet*
512 *Requests for Comments*. **2017**, RFC 8018. Available online: <https://tools.ietf.org/html/rfc8018> (accessed on 3
513 June 2019).
- 514 60. Visconti, A.; Bossi, S.; Ragab, H.; Calò, A. On the weaknesses of PBKDF2. In *Cryptology and Network Security*,
515 Proceedings of the 14th International Conference, CANS 2015, Marrakesh, Morocco, 10 - 12 December 2015;
516 Reiter M., Naccache D., Eds.; Springer International Publishing: Switzerland, 2015; pp. 119–126.
- 517 61. Visconti, A.; Mosnáček, O.; Brož, M.; Matyáš, V. Examining PBKDF2 security margin—Case study of LUKS.
518 *Journ. of Inf. Sec. and Appl.* **2019**, *46*, 296–306.
- 519 62. Visconti, A.; Gorla, F. Exploiting an HMAC-SHA-1 optimization to speed up PBKDF2. *IEEE Transactions on*
520 *Dependable and Secure Computing*. **2018**.
- 521 63. Biryukov, A.; Dinu, D.; Khovratovich, D. Argon2 (version 1.2) Cited 13 Nov 2018. Available online:
522 <https://password-hashing.net/submissions/specs/Argon-v3.pdf> (accessed on 28 May 2019).
- 523 64. Percival, C.; Josefsson, S. The scrypt Password-Based Key Derivation Function. *Internet Requests for Comments*.
524 **2016**, RFC 7914, 16. Available online <https://tools.ietf.org/html/rfc7914> (accessed on 30 May 2019).
- 525 65. Banks, A.; Gupta, R. MQTT Version 3.1.1 Plus Errata 01. Available online:
526 <http://docs.oasis-open.org/mqtt/mqtt/v3.1.1/mqtt-v3.1.1.html> (accessed on 24 May 2019).
- 527 66. Light, R. A. Mosquitto: server and client implementation of the MQTT protocol. *J. Open Source Software*.
528 **2017**, *2*, 265–265.

529 © 2019 by the authors. Submitted to *Symmetry* for possible open access publication
530 under the terms and conditions of the Creative Commons Attribution (CC BY) license
531 (<http://creativecommons.org/licenses/by/4.0/>).